Coupling of eruptions and earthquakes at Mt. Etna (Sicily, Italy): A case study from the 1981 and 2001 events

Stefano Gresta,[1] Francesca Ghisetti,[1,2] Eugenio Privitera,[3] and Amalia Bonanno[1,3]

[1]   Changes in Coulomb failure stress (ΔCFS) induced by dike propagation during two flank eruptions on Mt. Etna (1981 and 2001) are calculated for the most seismically active faults on the east slope of the volcano (the right-lateral Timpe fault system, oriented NNW-SSE, and the left-lateral Pernicana fault, oriented E-W). Calculations performed using Coulomb 2.5 software indicate that intrusion of a NNW dike on the NW side of the volcano (1981 eruption) rises ΔCFS on both the Timpe and Pernicana faults. In contrast, intrusion of a N-S dike at high elevation on the south flank (2001 eruption) rises ΔCFS only on Timpe fault System. These results are compatible with the observed pattern of seismicity, but emphasize an extremely heterogeneous state of stress on the east flank of the volcano. **Citation:** Gresta, S., F. Ghisetti, E. Privitera, and A. Bonanno (2005), Coupling of eruptions and earthquakes at Mt. Etna (Sicily, Italy): A case study from the 1981 and 2001 events, Geophys. Res. Lett., 32, L05306, doi:10.1029/2004GL021479.

1. Introduction

[2]   Earthquakes and eruptions are often coupled. In fact, earthquakes may trigger eruptions by modifying the state of stress in magma systems and, conversely, large magma intrusions change stress conditions in the volcanic edifice, eventually inducing earthquakes [Hill et al., 2002; Stein, 2003; Walter and Amelung, 2004].

[3]   Different studies show a correlation between sectors with a positive increase of Coulomb failure stress (less than 3 bars) and areas with increased rates of seismicity [e.g., Reasenberg and Simpson, 1992; Stein, 2003]. Triggering exerted by magmatic intrusions may extend for several months to years.

[4]   In this paper we examine two flank eruptions at Mt. Etna (March 1981 and July–August 2001) in terms of related stress field perturbations. The 1981 and 2001 eruptions offer good case histories because: i) dike propagation occurred with different orientation in two distinct regions of the volcano; ii) ground deformation is documented by a good quality data set; iii) quantitative models of the intrusive bodies are well-constrained [Bonaccorso, 1999; Bonaccorso et al., 2002]; iv) seismic activity on the east flank of the volcano occurred in the same time window of the eruptions.

[5]   Coulomb failure stress changes induced by these eruptions are analyzed for two of the most active faults on the eastern flank of Mt. Etna: the Timpe Fault system (TFS) and the Pernicana Fault (PF) (Figure 1).

[6]   TFS is defined by sets of ∼NNW-SSE, en-echelon faults, dipping 70° east, that control the steep Ionian coastline for more than 30 km (Figure 1). Progressive offset of superposed lava flows and geomorphic features record a history of late Pleistocene and Holocene motion with slip rates ≤2 mm/year [cf. Monaco et al., 1997]. Striated fault planes and coseismic slip during historical earthquakes indicate transtensional, right-lateral mechanisms. PF is an E-W, sub-vertical fault, extending from elevations of ∼1850 m down to the coastline, with a total length of ∼20 km along strike [Neri et al., 2003]. Offset of volcanic bodies, buildings and roads indicate left-lateral, transtensional slip at extremely fast slip rates (<13 mm/year) [Azzaro, 1997, 1999; Monaco et al., 1997]. Only the western segment of PF is seismically active, whereas creep prevails in the east (Figure 1).

[7]   On both faults the largest earthquakes (M ≤ 4.5) are extremely shallow (h ≤ 2 km), producing coseismic ground fracturing that results in strong ground shaking over small, (less than 1 km^2), but densely populated, areas.

2. Stress Field at Mt. Etna

[8]   Mt. Etna is a composite volcano located in the footwall of a system of seismically active faults that bound the east coast of Sicily for an overall length greater than 200 km. A sub-horizontal σ_1 oriented NNW-SSE is documented for the late Pliocene episodes of compression in the Sicilian thrust belt [Ghisetti, 1979], but the extent to which the Quaternary edifice of Mt. Etna sits in a compressive or rather in an extensional setting remains controversial [Monaco et al., 1997; Doglioni et al., 2001].

[9]   Part of the problem is that in a complex, tectono-volcanic setting like that of Mt. Etna, the stress field is likely to be extremely heterogeneous. In fact, stress components related to ascent and emplacement of magma induce time- and depth-dependent modifications of the "regional" stress field [Barberi et al., 2000]. In addition, the strong elevation gradients, and the large-scale sliding of the volcano eastern flank [Borgia et al., 1992] may strongly modify the local stress conditions.

[10]   Heterogeneity of the stress field at Mt. Etna is well documented by focal solutions of recent earthquakes that display a scatter in dip - from sub-horizontal to subvertical - of NNW-SSE oriented σ_1 axes (coupled to an E-W, sub-horizontal σ_3) [Barberi et al., 2000, 2004] and by the observed, contemporaneous activity of TFS and PF with

[1]Dipartimento di Scienze Geologiche, Università di Catania, Catania, Italy.
[2]Department of Geology, University of Otago, Dunedin, New Zealand.
[3]Istituto Nazionale di Geofisica e Vulcanologia - Sezione di Catania, Italy.
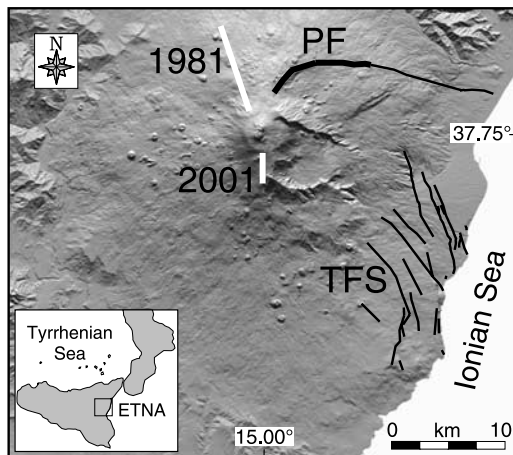
Figure 1. DEM of Mt. Etna volcano, showing the 1981 and 2001 eruptive fractures (white lines). Black lines indicate the Timpe fault system (TFS) and Pernicana fault (PF). The latter is divided in two segments, in bold the seismogenic one.

mechanisms (right and left-lateral, respectively) that are not compatible with any of the possible stress configurations.

3. Coulomb Stress

[11] The theory behind changes in Coulomb static stress failure (ΔCFS) and its application have been extensively described [e.g., *King et al.*, 1994]. $\Delta CFS = \Delta\tau_s + \mu(\Delta\sigma_n + \Delta P)$, where $\Delta\tau_s$ is the change in shear stress resolved in the direction of slip on a given fault plane, $\Delta\sigma_n$ is the change in normal stress along a direction normal to the fault plane, μ is the apparent coefficient of friction, and ΔP is the change in pore-fluid pressure. The indeterminacy of parameters like the fluid pressure [*Reasenberg and Simpson*, 1992] are resolved by assuming an effective coefficient of friction (μ') that includes the effects of pore fluids and the material properties of the fault zone. Thus: $\Delta CFS = \Delta\tau_s + \mu'\Delta\sigma_n$.

[12] Here we apply the software Coulomb 2.5 [*King et al.*, 1994] to study increased rates of seismic activity in a Magnitude range $2-4$ on two fault systems that are contemporaneously active, but possess a kinematics not compatible with the same orientation of the stress fields. This application allows us to investigate the effects of a range of input parameters on the stability of the solution in terms of positive correlation between an increase in ΔCFS and seismic activity. Concerning the material properties we have tested Young's modulus E from 60 to 100 GPa, coefficient of effective friction μ' between 0.2 and 0.6 and a Poisson's ratio $\nu = 0.25$. Various tests show that the results (excluding the boundaries of the lobes) are within the ranges $\pm 25\%$ and $\pm 35\%$ by varying E and μ', respectively. Here we use the average values E = 80 GPa, $\mu' = 0.4$.

[13] As discussed above, choice of the "regional" stress field is much more problematic in terms of dominant "regional" regime (strike-slip vs. normal) and long-term vs. short-term conditions controlled by episodic magmatic intrusions and gravitational instabilities.

[14] For these reasons we have tested the whole range of stress field orientations indicated by focal solutions (σ_1

oriented from N285° to N15° with a dip scatter 0°−90°) and we have explored the possibility of heterogeneous stress sources for TFS and PF. The inferred, eastward collapse of the volcano eastern flank adds another source of complexity on the stress field, but location, kinematics and geometry of the detachment surface are not univocally modeled [e.g., *Lundgren and Rosen*, 2003; *Puglisi and Bonforte*, 2004]. Thus, controversial results arise from alternative models. Though we are well aware of the limitations associated with simplified assumptions, here we present the results of ΔCFS calculations based on possible, but limited ranges of input parameters with: horizontal σ_1, oriented N337° and PF and TFS analysed for the cases of: *i*) "optimally oriented strike-slip faults"; or *ii*) specified faults (calculations are performed excluding regional stress field). In the latter case, PF is a receiver vertical plane oriented N95°, with rake 0° (left lateral) and TFS is a receiver plane oriented N337°, dipping 70°NE, with rake 180° (right lateral).

[15] The magmatic sources of the 1981 and 2001 eruptions have been modeled by using some different approaches [e.g., *Sanderson et al.*, 1983; *Lundgren and Rosen*, 2003]. Here we use the sources modeled by inversion of ground deformation data [*Bonaccorso*, 1999; *Bonaccorso et al.*, 2002].

[16] PF was only active during the 1981 eruption (both before and after) whereas TFS was active after both eruptions of 1981 and 2001. The largest earthquakes are listed in Table 1.

[17] For the 2001 earthquakes we used both macroseismic surveys and our computation of fault plane solutions, whereas for the 1981 earthquakes we used only the macrosesimic data of *Azzaro* [1999], due to a paucity of good quality onset polarities. The orientation and slip of PF and TFS that we have used in the modeling are in agreement with the seismic data.

[18] The depth interval of earthquakes is different for TFS ($0-4$ km b.s.l) and PF (2 km a.s.l−1 km b.s.l.). A series of test we have performed show no significant dependence of the results on this depth variations; consequently, we use an average value of 1.5 km b.s.l for TFS and 1 km a.s.l. for PF.

3.1. 1981 Eruption

[19] The 17th−23rd March 1981 eruption is the most important flank eruption on the northwest slope of Mt. Etna

Table 1. List of the Largest Earthquakes ($2.7 \leq M \leq 4.0$) That Occurred on TFS and PF (in Bold) Before and/or After the 1981 and 2001 Eruptions

	1981			2001	
#	Data	M	#	Data	M
1	**Jan-04**	**4.0**	1	Aug-30	2.9
2	**Mar-24**	**2.8**	2	Sep-26	2.9
3	Apr-30	3.5	3	Oct-15	2.7
4	Jul-03	3.3	4	Oct-18	2.8
5	Jul-07	2.9	5	Oct-26	2.9
6	Jul-14	3.0	6	Oct-28 (09:03)	3.5
7	Jul-19	2.9	7	Oct-28 (11:00)	2.8
8	Jul-29	3.2	8	Oct-28 (15:05)	3.2
9	Sep-01	3.6	9	Oct-31	2.8
10	Sep-02	2.9			
11	Sep-13	3.3			
12	Oct-10	2.9			
13	**Oct-11**	**2.9**			
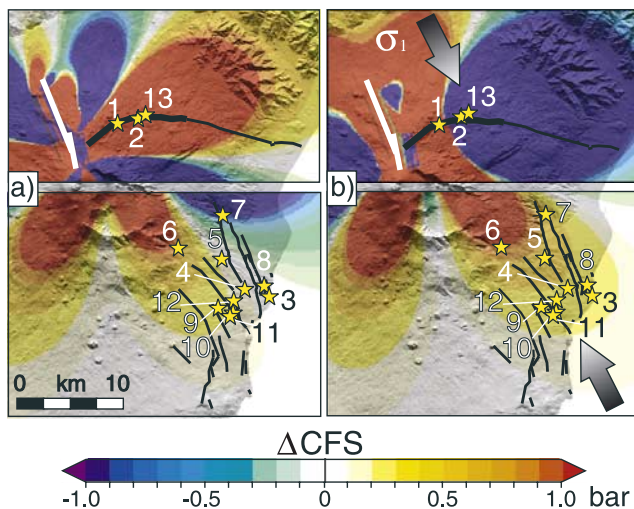
Figure 2. ΔCFS induced by the 1981 dike intrusions in the NW flank (white lines). Stars indicate earthquake epicenters (numbers as in Table 1). (a) Specified fault calculation: (top) ΔCFS is shown for an average depth of 1 km a.s.l.; and (bottom) ΔCFS is calculated at 1.5 km b.s.l. (b) The same as in Figure 2a but including regional stress field (σ_1 = N337°; grey arrows) in computation (optimally oriented strike-slip faults: right-lateral = N303°, left-lateral = N16°).

in the last century. According to *Bonaccorso* [1999] ground deformation indicates that the dike intrusions started 3–4 months before the eruption. The eruption began with a NNW-SSE oriented, northward propagating fracture that broke 7 km downslope (from 2500 to 1100 m a.s.l., Figure 1), in about 6 hs. Most of the lava was erupted at high rates (~35 m³/s) in the first 20 hs. The estimated total magma output ranges between 18×10^6 and 25×10^6 m³.

[20] In our calculations we have assumed the double tensile crack model of the eruptive fissure of *Bonaccorso* [1999]. Accordingly, the first and deeper crack (NNW-SSE oriented, west-dipping and 5 m wide) radiated from the summit of the volcano, from ~1700 to 300 m a.s.l., for an extent of ~3 km. The second, shallower crack (NNW-SSE oriented, west-dipping and 1 m wide) propagated north for 7 km.

[21] In our Coulomb 2.5 calculations the double dike intrusions are treated as "uniform dislocations in a homogeneous elastic half-space". For the case of "specified fault" we obtain: *i*) a strong increase of ΔCFS (greater than 13 bar) in the seismogenic segment of PF (Figure 2a, top); *ii*) a slight increase (0.1–0.2 bar) of ΔCFS on part of TFS (Figure 2a, bottom). For the case of "optimally oriented fault" we obtain: *iii*) a decrease of ΔCFS (~−1.0 bar) on the optimally oriented planes in most of the area affected by the seismogenic segment of PF (Figure 2b, top); *iv*) an increase of ΔCFS (0.1–0.9 bar) for the optimally oriented (N303°, vertical) right-lateral strike-slip faults in the whole area surrounding TFS that was affected by increased seismic activity (Figure 2b, bottom).

3.2. 2001 Eruption

[22] The July 17th–August 9th, 2001 flank eruption of Mt. Etna was characterized by an extremely high volume of ejected pyroclastic material, nearly equal to the lava volume

(~50×10^6 m³). The eruptive setting was rather complex, with involvement of the southeast summit crater and flank fractures. The main eruptive fracture propagated with N-S trend for about 7 km (Figure 1), extending from 3000 to 2100 m a.s.l.

[23] Inversion of ground deformation data is compatible with intrusion of a 2.2 km long, 3.5 m wide dike trending N7° that propagated southeast of the summit craters, from elevations of 1400 m a.s.l. to 900 m b.s.l. [*Bonaccorso et al.*, 2002]. For the case of "specified fault" we obtain: *i*) negative ΔCFS (down to −2 bar) on the potentially seismogenic segments of PF (Figure 3a, top); *ii*) a decrease of ΔCFS (down to −1 bar) on almost the whole length of TFS (Figure 3a, bottom). For the case of "optimally oriented fault" we obtain: *iii*) an increase of ΔCFS (up to 3 bar) on the optimally oriented planes in most of the area crossed by the seismogenic segment of PF (Figure 3b; top); *iv*) an increase of ΔCFS (0.5–5.0 bar) on the optimally oriented right-lateral strike-slip faults (N303°, vertical), in the TFS area (Figure 3b, bottom). All the largest earthquakes (2.7 ≤ M ≤ 3.5) that occurred in the four months following the end of the eruption (Table 1) are located in the area of increased ΔCFS around TFS, and the fault plane solutions are compatible with the orientation of the computed optimally oriented faults. No earthquakes occurred on PF during the period August 2000–August 2002.

4. Discussion

[24] Calculations of ΔCFS performed using Coulomb 2.5 software are obviously dependent on the choice of the input parameters, with some assumptions having stronger weight than others. We have presented solutions based on a limited range of input parameters, though we actually tested the sensitivity of results to a wide range of conditions. Our model calculations suggest that the interaction between flank eruptions at Mt. Etna and earthquakes on TFS and PF is complex, but feasible. Causes of complexities are multiple. Material properties are likely to be heterogeneous,
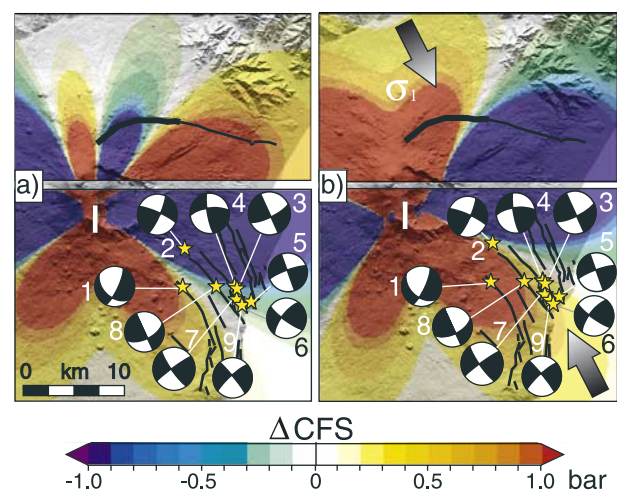
Figure 3. ΔCFS induced by the 2001 dike intrusion in the south slope (white line). Earthquake epicenters (stars) are plotted together with lower hemisphere projection of fault plane solutions (numbers as in Table 1). Same assumptions as in Figure 2.

especially considering the fabric of the fault zones relative to the surrounding rocks, and the strong variations in heat flow and fluid pressure during eruptive cycles. Different values of E and μ' do not alter the shape and size of the lobes of increased stress, but affect the magnitude of ΔCFS up to about 35%. Given the low magnitude of the observed earthquakes, even small changes in ΔCFS are likely to affect seismicity.

[25] However, we feel that the parameter that mostly influences our solutions is the stress field. We have tested conditions that either exclude or include the regional stress field. In the latter case we have chosen a regional strike-slip stress field with σ_1 sub-horizontal $\sim$N-S and σ_3 sub-horizontal, $\sim$E-W. This choice fits a large number of earthquake focal solutions in the investigated area, and is validated by the right-lateral movement on TFS, but is at odds with left-lateral movement on PF.

[26] Our computations (Figures 2 and 3) show that: i) intrusion of NNW-SSE dikes in the north-west flank of Mt. Etna (as in 1981) rises ΔCFS on "optimally oriented" faults and may determine a strong increase on PF, but only in the case of "specified fault" (Figures 2a, top and 2b, bottom); ii) intrusion of N-S dikes in the south flank (as in 2001) increases ΔCFS only on the "optimally oriented" faults, and specifically decreases ΔCFS on PF in the case of "specified fault".

[27] These results suggest that PF needs specific driving mechanisms other than the regional stress field.

[28] The seismicity recorded both on 1981 and 2001 in the area of TFS has occurred on fault segments striking from N318° to N337°. This matches with the strike of optimally oriented right-lateral strike-slip faults (N303°, vertical).

[29] A different behavior between PF and TFS is evidenced. Dike intrusions with favorable orientation trigger earthquakes on PF, but barely encourage earthquakes on TFS.

[30] We have evidenced a strongly heterogeneous stress field, as a possibly consequence of transient dynamic changes in shear stress, fluid pressure and dynamic slope instabilities, all mainly controlled by magmatic intrusions. A refinement of our simple approach will certainly require a more sophisticated modeling of the sources that eventually includes the effect of the collapse of the east flank above a basal detachment.

[31] However, our results make sense of i) the observed seismic activity along TFS during both 1981 and 2001, ii) the significant seismic activity on PF before (at the start of dike intrusion?) and after the March 1981 eruption, iii) no seismic activity on PF during the whole 2001.

5. Conclusions

[32] Changes in Coulomb failure stress calculated for the 1981 and 2001 flank eruptions at Mt. Etna are compatible with the observed seismic activity, from some months before the eruption to some months after, on the east slope of the volcano. However, increase of seismic activity on the two largest faults of the volcano (TFS and PF) cannot be modeled within a homogeneous stress field, and appears to depend on location and orientation of the magmatic fractures.

[33] Stress perturbation driven by emplacement of extensional magma-driven dikes may trigger and/or encourage rupturing at shallow depth of fault segments. Though small (M $\leq$ 4.5), these earthquakes have a severe impact on the infrastructure of the densely populated east slope of the volcano.

References

Azzaro, R. (1997), Seismicity and active tectonics along the Pernicana Fault, Mt. Etna (Italy), *Acta Vulcanol.*, 9, 7–14.

Azzaro, R. (1999), Earthquake surface faulting at Mount Etna volcano (Sicily) and implications for active tectonics, *J. Geodyn.*, 28, 193–213.

Barberi, G., O. Cocina, G. Neri, E. Privitera, and S. Spampinato (2000), Volcanological inferences from seismic strain tensor computations at Mt. Etna Volcano, Sicily, *Bull. Volcanol.*, 62, 318–330.

Barberi, G., O. Cocina, V. Maiolino, C. Musumeci, and E. Privitera (2004), Insight into Mt. Etna (Italy) kinematics during the 2002–2003 eruption as inferred from seismic stress and strain tensors, *Geophys. Res. Lett.*, 31, L21614, doi:10.1029/2004GL020918.

Bonaccorso, A. (1999), The 1981 March Mt. Etna eruption inferred through ground deformation modelling, *Phys. Earth Planet. Inter.*, 112, 125–136.

Bonaccorso, A., M. Aloisi, and M. Mattia (2002), Dike emplacement fore-running the Etna July 2001 eruption modeled through continuous tilt and GPS data, *Geophys. Res. Lett.*, 29(13), 1624, doi:10.1029/2001GL014397.

Borgia, A., L. Ferrari, and G. Pasquarè (1992), Importance of gravitational spreading in the tectonic and volcanic evolution of Mount Etna, *Nature*, 357, 231–235.

Doglioni, C., F. Innocenti, and G. Mariotti (2001), Why Mt. Etna?, *Terra Nova*, 13, 25–31.

Ghisetti, F. (1979), Relazioni tra strutture e fasi trascorrenti e distensive lungo i sistemi Messina-Fiumefreddo, Tindari-Letojanni e Alia-Malvagna (Sicilia nord-orientale): Uno studio microtettonico (in Italian), *Geol. Romana*, 18, 23–58.

Hill, D. P., F. Pollitz, and C. Newhall (2002), Earthquake-volcano interactions, *Phys. Today*, 55, 41–47.

King, G. C. P., R. S. Stein, and J. Lin (1994), Static stress changes and the triggering of earthquakes, *Bull. Seismol. Soc. Am.*, 84, 935–953.

Lundgren, P., and P. A. Rosen (2003), Source model for the 2001 flank eruption of Mt. Etna volcano, *Geophys. Res. Lett.*, 30(7), 1388, doi:10.1029/2002GL016774.

Monaco, C., P. Tapponnier, L. Tortorici, and P. Y. Gillot (1997), Late Quaternary slip rates on the Acireale-Piedimonte normal faults and tectonic origin of Mt. Etna (Sicily), *Earth Planet. Sci. Lett.*, 147, 125–139.

Neri, M., V. Acocella, and B. Behncke (2003), The role of the Pernicana Fault system in the spreading of Mt. Etna (Italy) during the 2002–2003 eruption, *Bull. Volcanol.*, 66, doi:10.1007/s00445-003-0322-x.

Puglisi, G., and A. Bonforte (2004), Dynamics of Mount Etna Volcano inferred from static and kinematic GPS measurements, *J. Geophys. Res.*, 109, B11404, doi:10.1029/2003JB002878.

Reasenberg, P. A., and R. W. Simpson (1992), Response of regional seismicity to the static stress change produced by the Loma Prieta earthquake, *Science*, 255, 1687–1690.

Sanderson, T. J. O., G. Berrino, G. Corrado, and M. Grimaldi (1983), Ground deformation and gravity changes accompanying the March 1981 eruption of Mount Etna, *J. Volcanol. Geotherm. Res.*, 16, 299–315.

Stein, R. S. (2003), Earthquake conversations, *Sci. Am.*, 288, 72–79.

Walter, T. R., and F. Amelung (2004), Influence of volcanic activity at Mauna Loa, Hawaii, on earthquake occurrence in the Kaoiki Seismic Zone, *Geophys. Res. Lett.*, 31, L07622, doi:10.1029/2003GL019131.

————————————

A. Bonanno, F. Ghisetti, and S. Gresta, Dipartimento di Scienze Geologiche, Università di Catania, Palazzo delle Scienze, Corso Italia, 55, Catania I-95129, Italy. (gresta@unict.it)

E. Privitera, Istituto Nazionale di Geofisica e Vulcanologia - Sezione di Catania, Piazza Roma 2, Catania I-95123, Italy.